Journal of Alloys and Compounds 509 (2011) L284–L288

Contents lists available at ScienceDirect

Journal of Alloys and Compounds

journal homepage: www.elsevier.com/locate/jallcom

Letter

Polymorphic phase transition-induced electrical behavior of $BiCoO_3$-modified $(K_{0.48}Na_{0.52})NbO_3$ lead-free piezoelectric ceramics

Wenjuan Wu, Dingquan Xiao*, Jiagang Wu, Wenfeng Liang, Jing Li, Jianguo Zhu

Department of Materials Science, Sichuan University, Chengdu 610064, PR China

ARTICLE INFO

Article history:
Received 24 February 2011
Received in revised form 28 April 2011
Accepted 2 May 2011
Available online 7 May 2011

Keywords:
Alkali niobate
BiCoO3
Polymorphic phase transition (PPT)
Dielectric properties

ABSTRACT

$(1-x)(K_{0.48}Na_{0.52})NbO_3$-$x$BiCoO$_3$ [KNN-xBC] lead-free piezoelectric ceramics were prepared by the conventional solid-state sintering method. The effects of the $BiCoO_3$ addition on the phase structure, dielectric, piezoelectric and ferroelectric properties of KNN-xBC ceramics were systematically investigated. The polymorphic phase transition (PPT) from rhombohedral to orthorhombic phase around room temperature was identified in the composition range of $0.01 \leq x \leq 0.02$, and the improved electrical properties were induced by this PPT. The KNN-0.01BC ceramics near PPT exhibit optimum electrical properties: $d_{33} \sim 165$ pC/N, $k_p \sim 0.40$, $P_r \sim 31.0\ \mu C/cm^2$, and $E_c \sim 12.6$ kV/cm. These results indicate that the enhanced piezoelectric properties for alkali niobate can be achieved by forming the coexistence of rhombohedral and orthorhombic phases.

1. Introduction

Perovskite-type structure $(K_{0.5}Na_{0.5})NbO_3$ (KNN)-based ceramics have been considered a promising candidate for lead-free piezoelectric ceramics because of its excellent piezoelectric properties, high Curie temperature, and environmental friendliness [1]. The ceramics undergo successive polymorphic phase transitions with temperature: rhombohedral to orthorhombic (R–O) transition at −123 °C, orthorhombic to tetragonal (O–T) transition at 200 °C, and tetragonal to cubic (T–C) transition at 410 °C, respectively [2,3]. It is well known that the polymorphic phase transition (PPT) plays an important role in the dielectric and piezoelectric properties of KNN ceramics [4–6]. A great deal of researchers have recently reported that the doping additives might have different effects on the temperature of the phase transition, and then the improvement in piezoelectric properties of KNN ceramics can be achieved by shifting the orthorhombic to tetragonal (O–T) PPT around room temperature [4–10]. In contrast, the R–O phase transition temperature (T_{R-O}) at a low temperature has been almost neglected for the KNN system. More recently, it has been reported that the T_{R-O} phase transition below room temperature of (Na, K) (Nb, Sb) O_3, KNN-$BaZrO_3$ and KNN-$BiScO_3$ ceramics can be tuned close to room temperature, and better piezoelectric properties are induced by the theory of two-phase coexistence [11–13].

Perovskite type Bi-based ferroelectrics of $BiMeO_3$ have a strong ferroelectricity and a high Curie temperature, where the giant electric polarization of $\sim 150\ \mu C/cm^2$ is predicted for $BiCoO_3$ by using the first-principles Berry-phase method [14]. It has been also shown that the addition of $BiCoO_3$ is of great value to improve the piezoelectric properties of $Bi_{0.5}Na_{0.5}TiO_3$–$Bi_{0.5}K_{0.5}TiO_3$ ceramics [15]. However, there are no systematic investigations on the solid solution of KNN–$BiCoO_3$ ceramics till now.

In the present work, $(1-x)(K_{0.48}Na_{0.52})NbO_3$-$x$BiCoO$_3$ [KNN-xBC] lead-free piezoelectric ceramics were prepared by the conventional sintering technique. The objective of the present study is to investigate the effects of the $BiCoO_3$ addition on the phase structure and electrical properties of KNN-xBC ceramics. The improvement in electrical properties of KNN-xBC ceramics is induced by shifting the rhombohedral to orthorhombic phase transition around room temperature.

2. Experimental

$(1-x)(K_{0.48}Na_{0.52})NbO_3$-$x$BiCoO$_3$ [KNN-xBC] (x = 0, 0.005, 0.0075, 0.01, 0.0125, 0.015, 0.02, 0.03, and 0.04, respectively) ceramics were prepared by the conventional solid-state reaction technique, where K_2CO_3 (99%), Na_2CO_3 (99.8%), Nb_2O_5 (99.5%), Bi_2O_3 (99%), and Co_2O_3 (99%) were used as starting raw materials. The stoichiometric powders were mixed by the ball milling for 24 h with zirconia balls media in anhydrous ethanol, and then dried. The dried powders were calcined at ~850 °C for 6 h, and the calcined powders were pressed into disks at ~20 MPa using polyvinyl alcohol (PVA) as a binder with diameters of ~10 mm and thicknesses of ~0.8–1.0 mm. After burning off PVA, the ceramic disks were sintered in the temperature range of 1110–1130 °C for 2 h in air. Silver paste was sintered on both sides of the specimens at ~700 °C for 10 min to form electrodes for the dielectric and piezoelectric measurements. The specimens were poled in a silicon oil bath at 120 °C by applying a dc electric field of 4.5 kV/mm for 30 min. All the electrical measurements were conducted on aged specimens (24 h after poling).

---

* Corresponding author. Tel.: +86 28 854 124 15; fax: +86 28 85 415 045.
E-mail address: nic0402@scu.edu.cn (D. Xiao).

0925-8388/$ – see front matter © 2011 Elsevier B.V. All rights reserved.
doi:10.1016/j.jallcom.2011.05.004

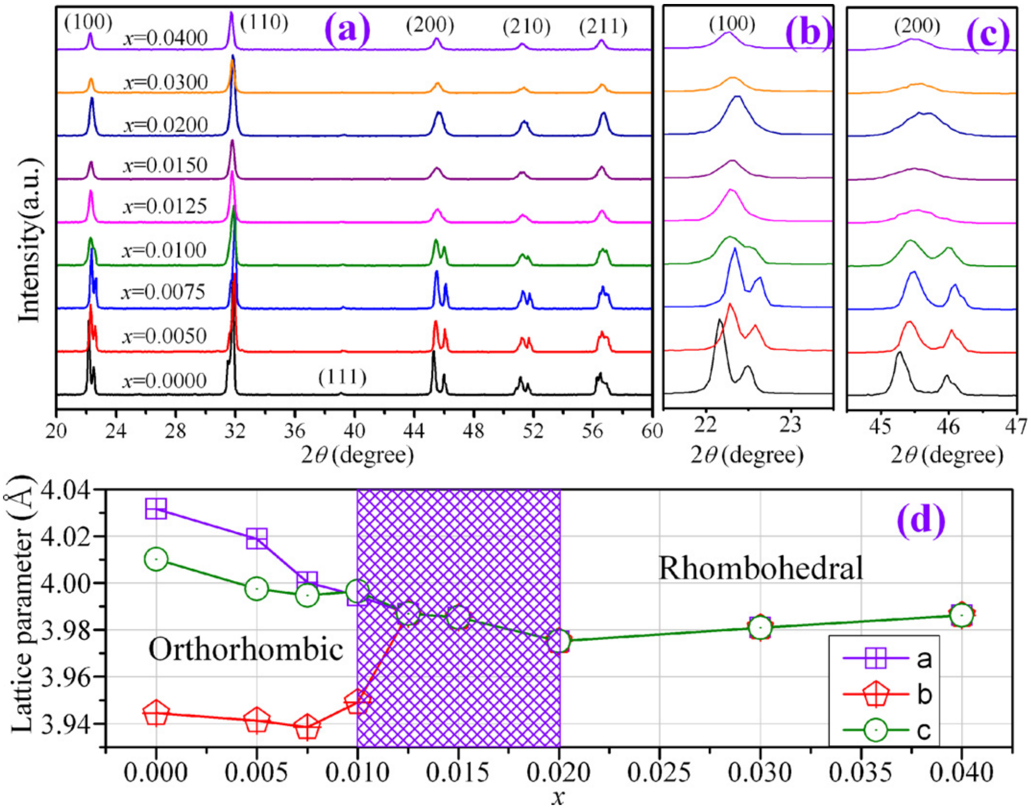

Fig. 1. (a) XRD patterns of KNN-*x*BC ceramics as a function of *x*, and enlarged XRD patterns in the 2θ ranges of (b) 21.5–23.5° and (c) 44.5–47° (d) The variation of lattice parameters as a function of x.

The crystal structure of the specimens was examined by the X-ray diffraction (XRD) using Cu Kα radiation (λ = 1.54178 Å) in the θ–2θ scan mode (DX1000, Dandong, China). Their piezoelectric constant (d_{33}) was measured using a piezo-d_{33} meter (ZJ-3A, China). Their electromechanical coupling factor k_p were determined by an precision impedance analyzer (Agilent 4294A, Santa Clara, CA) using the resonance–antiresonance technique. The dielectric constant as a function of temperature was obtained using an *LCR* meter (HP 4980, Agilent, USA). The polarization versus electric field (*P*–*E*) hysteresis loops of the ceramics were measured using a Radiant Precision Workstation (USA).

3. Results and discussions

Fig. 1(a) shows the XRD patterns of KNN-*x*BC ceramics as a function of *x*. All ceramics are of a single-phase perovskite structure, and no secondary phases are observed in the range detected, indicating that the $BiCoO_3$ can completely diffuse into KNN lattices to form stable KNN-*x*BC solid solutions in the range of compositions investigated. Fig. 1(b) and (c) plot the enlarged XRD patterns for the KNN-*x*BC ceramics in the 2θ ranges of 21.5–23.5° and 44.5–47°. The pure KNN ceramic has an orthorhombic structure at room temperature, as indicated by the splitting of (2 0 0) and (1 0 0) peaks [3]. The KNN-*x*BC ceramics with $x < 0.01$ still maintain the orthorhombic structure. With further increase of the BC content ($x > 0.02$), the ceramics are of a rhombohedral structure, where the split (2 0 0) and (1 0 0) peaks gradually emerge into a single peak. These results indicate that a coexistence of orthorhombic and rhombohedral structures is formed at room temperature in the composition range of $0.01 \le x \le 0.02$, where the (2 0 0) and (1 0 0) peaks are broader than that of the rhombohedral structure. Fig. 1(d) gives the variation of lattice parameters as a function of *x*. The lattice parameters ($a \approx c$ and b) for an orthorhombic structure decrease with increasing the BC content ($x < 0.01$), and the lattice parameters ($a = c = b$) for the rhombohedral structure increase with further increasing the BC content ($x > 0.02$). However, the lattice parameters of KNN-*x*BC ceramics with $0.01 \le x \le 0.02$ have an obvious difference, further confirming the phase transitional behavior from orthorhombic to rhombohedral symmetry. A PPT between the orthorhombic and the rhombohedral phase should exist approximately at $0.01 \le x \le 0.02$. The following electrical characterization is also given to those compositions around PPT.

The dielectric constant of KNN-*x*BC ceramics as a function of temperature is measured at 10 kHz, as plotted in Fig. 2. Pure KNN ceramic has two-phase transition temperatures, corresponding to the ferroelectric orthorhombic–tetragonal polymorphic phase

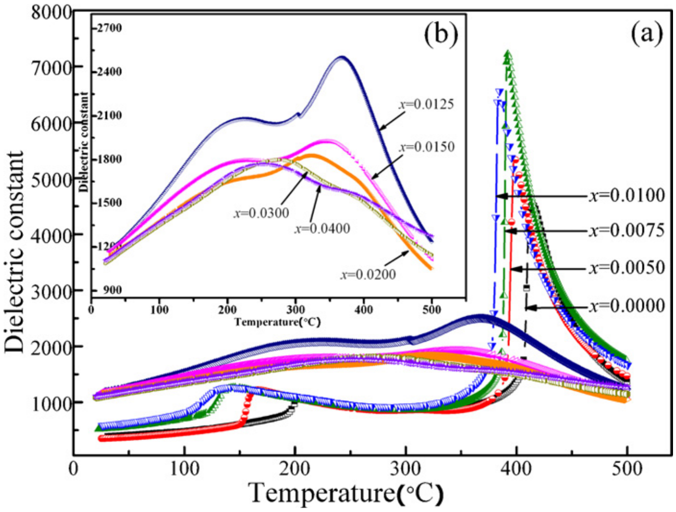

Fig. 2. (a) Dielectric constant (ε_r) at 10 kHz as function of varied temperature for the KNN-*x*BC ceramics, and (b) the magnified dielectric constant vs. temperature curves only for samples with *x* = 0.0125–0.04.

transition (T_{O-T}) at ~204 °C and the tetragonal–cubic transition (T_C) at ~414 °C [2]. With increasing the BC content ($x < 0.01$), both of phase transition temperatures simultaneously shift to a lower temperature. In contrast, the KNN-*x*BC ceramics with $0.01 \leq x \leq 0.02$ exhibit two broad and abnormal dielectric peaks, corresponding to the O–T and T–C phase transitions. At $x = 0.03$, the orthorhombic–tetragonal phase transition disappears, and the ceramic possesses a solely rhombohedral structure, as shown in Fig. 2(b). This result confirms that the ceramics with the compositions of $0.02 < x \leq 0.04$ are of rhombohedral ferroelectrics, not cubic paraelectrics, which is consistent with the XRD analysis. Moreover, it is noticeable that the ceramics with a rhombohedral phase show a higher dielectric peak and a broader phase transition as compared to those of the ceramics with an orthorhombic phase, and such behavior may originate from a more complex occupation of A and B sites in the ABO_3 perovskite structure.

In order to further analyze the phase structure, the dielectric constant of KNN-0.01BC and KNN-0.015BC ceramics versus temperature at heating and cooling cycles was measured, as shown in Fig. 3. The ceramics with $x = 0.01$ possess a rhombohedral phase from −30 °C, and the orthorhombic phase appears with increasing the temperature, indicating the coexistence of rhombohedral and orthorhombic (R&O) phases at room temperature. By comparison, the several ferroelectric phases (R, O, and T) of KNN-0.015BC ceramics slightly shift to a higher temperature, whereas the KNN-0.015BC ceramics still possess the coexistence of R&O phases at room temperature. According to the above mentioned results, the coexistence of R&O phases is formed for the KNN-*x*BC ceramics with the composition of $0.01 \leq x \leq 0.02$ near room temperature.

Furthermore, the XRD patterns of KNN-0.01BC ceramics at different temperatures were measured in order to confirm the phase transitional behavior of the ceramics, which is shown in Fig. 4. Fig. 4 indicates that the phase structure of KNN-0.01BC ceramics exhibits the coexistence of R&O phases at ~25 °C, and approaches the orthorhombic phase. The ceramics undergo a transform from orthorhombic to tetragonal phase, then to a cubic phase with rising measurement temperature. In addition, it can be observed that the ceramics possess the coexistence of the orthorhombic and tetragonal phases at 100–120 °C, which is in accordance with the temperature dependence of the dielectric constant of the ceramics.

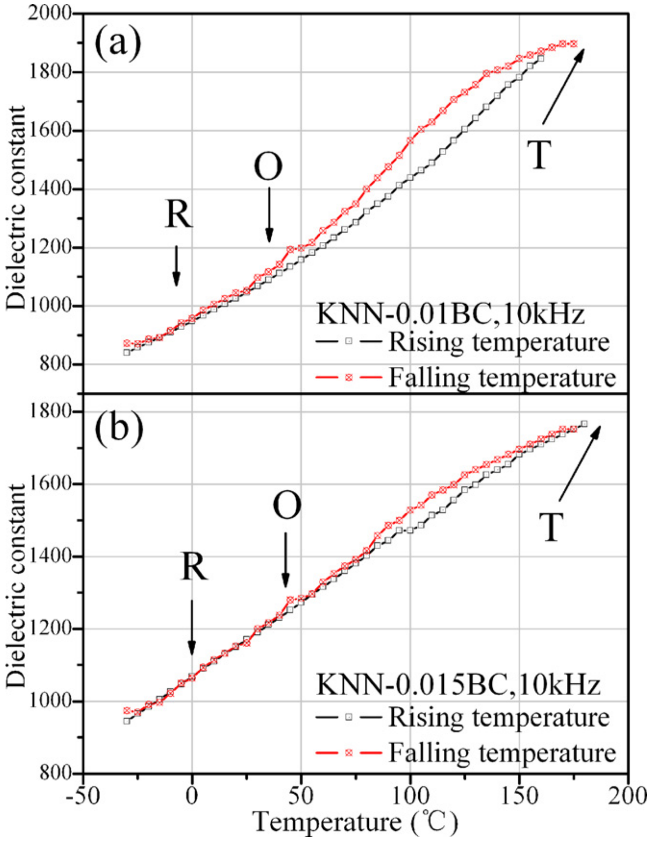

Fig. 3. Dielectric constant at 10 kHz as function of varied temperature (from −30 to 180 °C) for (a) KNN-0.01BC and (b) KNN-0.015BC ceramics for both rising and falling temperature cycles.

Fig. 5 shows the *P*–*E* hysteresis loops of KNN-*x*BC ceramics, measured at room temperature and the frequency of 20 Hz. It can be

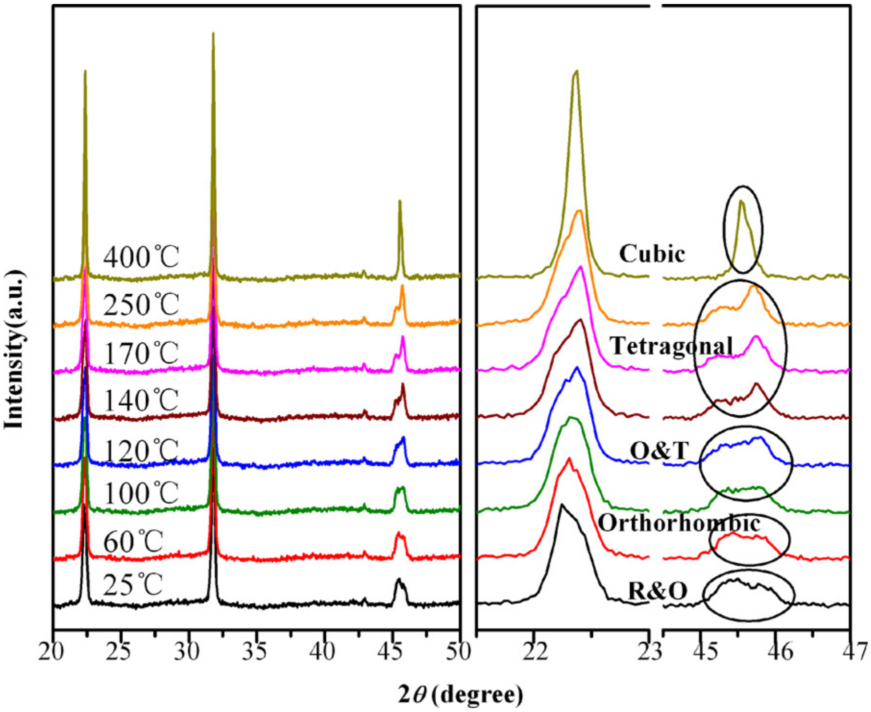

Fig. 4. XRD patterns for the KNN-0.01BC ceramic at different temperatures.

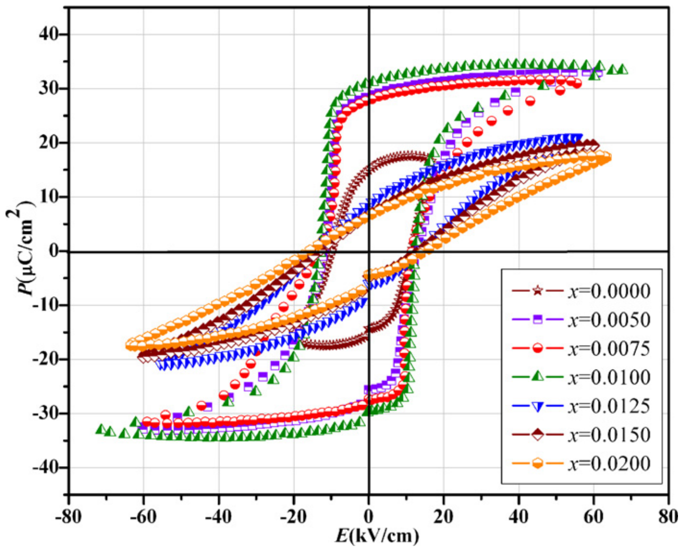

Fig. 5. *P*–*E* hysteresis loops of KNN-*x*BC ceramics at room temperature.

observed that the ferroelectric properties strongly depend on their compositions. The *P*–*E* curve for pure KNN ceramic shows roundish due to a high leakage current density, and the ferroelectricity firstly enhances and then weakens with increasing the BC content. The KNN-0.01BC ceramics exhibit the best ferroelectric properties with a remnant polarization of $P_r \sim 31.0\ \mu C/cm^2$ and a coercive field of $E_c \sim 12.6$ kV/cm, indicating a higher degree of orientation of the ferroelectric domain near the PPT composition.

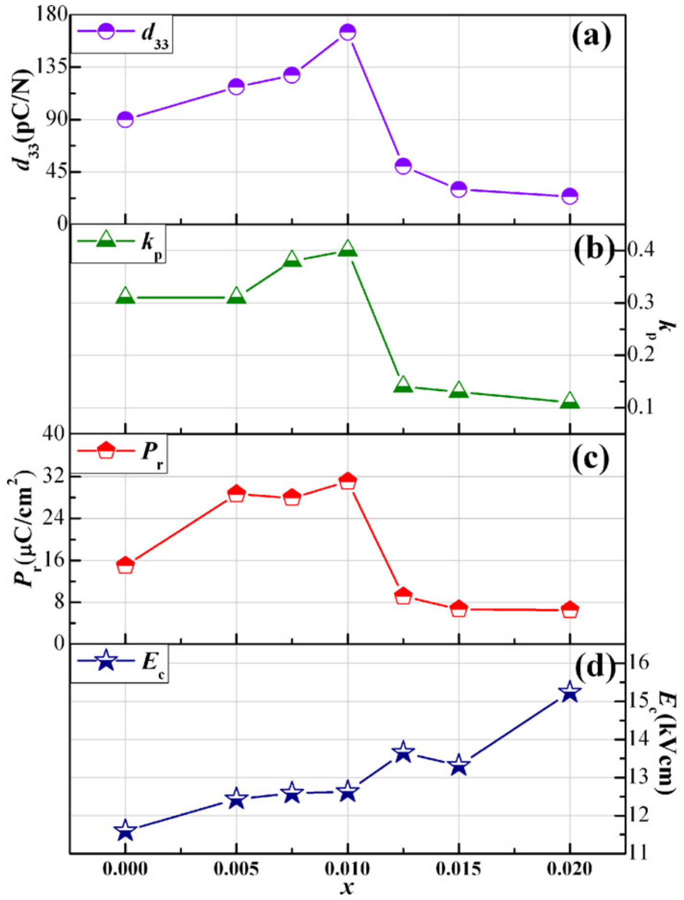

Fig. 6. Compositional dependence of (a) piezoelectric coefficient d_{33}, (b) electromechanical coupling factor k_p, (c) remnant polarization P_r, and (d) coercive field E_C at room temperature of KNN-*x*BC ceramics.

Fig. 6(a) and (b) shows the compositional dependence of the piezoelectric coefficient (d_{33}) and electromechanical coupling factor (k_p) of KNN-*x*BC ceramics. The d_{33} and k_p values greatly increase with the addition of $BiCoO_3$, and then rapidly decrease with further increasing the addition of $BiCoO_3$. The best piezoelectric properties with $d_{33} \sim 165$ pC/N and $k_p \sim 0.40$ appear in the composition with $x = 0.01$. These results indicate that the 0.99KNN-0.01BC ceramic possesses optimum piezoelectric properties at room temperature owing to the PPT at room temperature and a high content of orthorhombic phase. Fig. 6(c) and (d) give the remnant polarization (P_r) and the coercive field (E_C) at room temperature as a function of the addition amount of BC. As seen from Fig. 6(c), the P_r value of the ceramics increases from $\sim 15.0\ \mu C/cm^2$ to $\sim 31.0\ \mu C/cm^2$, while the addition of BC at $x > 0.1$ weakens the ferroelectricity of the ceramics. The E_C value of the ceramics increases with the increase of BC addition, which may be attributed to the pinning effect of the domain walls for the ceramics due to the increase in the number of oxygen vacancies generated by addition of Co.

The perovskite ferroelectric oxides possess ferromagnetism as well as ferroelectric property at room temperature by introducing the transition-metal magnetic elements (Fe, Co) [16,17], such as Fe-doped $PbTiO_3$ [14], and Co-doped $(Na_{0.5}Bi_{0.5})TiO_3$ [17]. Therefore, it is of great interest to research the ferromagnetism of the KNN-*x*BC ferroelectric ceramics by doping magnetic elements (Co). Our preliminary results show that the KNN-*x*BC ceramics exhibit a weak ferromagnetic order at room temperature, and the detailed researches are in hand and the results will be published in another paper.

4. Conclusion

Lead-free piezoelectric ceramics $(1-x)(K_{0.48}Na_{0.52})NbO_3$-$xBiCoO_3$ [KNN-*x*BC] were prepared by the conventional solid-state sintering method, and the effects of the $BiCoO_3$ addition on the phase structure and electrical properties of KNN-*x*BC ceramics were investigated. The polymorphic phase transitions (PPT) from rhombohedral to orthorhombic phase around room temperature were identified in the composition range $0.01 \le x \le 0.02$. The KNN-0.01BC ceramics near the PPT possess optimum piezoelectric and ferroelectric properties: $d_{33} \sim 165$ pC/N, $k_p \sim 0.40$, $P_r \sim 31.0\ \mu C/cm^2$, and $E_c \sim 12.6$ kV/cm. These results indicate that the enhanced piezoelectric properties can be achieved based on the coexistence of rhombohedral and orthorhombic phases.

Acknowledgements

This work was supported by National Science Foundation of China (NSFC nos. 50772068 and 50972001) and Foundation of Doctor Training Program in University and College in China (nos. 20030610035, and 20080610020).

References

[1] Y. Saito, H. Takao, T. Tani, T. Nonoyama, K. Takatori, T. Homma, T. Nagaya, M. Nakamura, Nature 432 (2004) 84.
[2] B. Jaffe, W.R. Cook, H. Jaffe, Piezoelectric Ceramics, Academic, New York, 1971, p115.
[3] L. Egerton, D.M. Dillon, J. Am. Ceram. Soc. 42 (1959) 438.
[4] S.J. Zhang, R. Xia, T.R. Shrout, G.Z. Zang, J.F. Wang, J. Appl. Phys. 100 (2006) 104108.
[5] J.G. Wu, Y.Y. Wang, D.Q. Xiao, J.G. Zhu, Z.H. Pu, Appl. Phys. Lett. 91 (2007) 132914.
[6] J.L. Zhang, X.J. Zong, L. Wu, Y. Gao, P. Zheng, S.F. Shao, Appl. Phys. Lett. 95 (2009) 022909.
[7] Y.P. Guo, K. Kakimoto, H. Ohsato, Appl. Phys. Lett. 85 (2004) 4121.
[8] J.G. Wu, D.Q. Xiao, Y.Y. Wang, J.G. Zhu, L. Wu, Y.H. Jiang, Appl. Phys. Lett. 91 (2007) 252907.

[9] H.L. Du, W.C. Zhou, F. Luo, D.M. Zhu, S.B. Qu, Y. Li, Z.B. Pei, J. Appl. Phys. 104 (2008) 344104.

[10] H.L. Du, D.J. Liu, F.S. Tang, D.M. Zhu, W.C. Zhou, S.B. Qu, J. Am. Ceram. Soc. 90 (2007) 2824.

[11] R.Z. Zuo, J. Fu, D.Y. Lv, Y. Liu, J. Am. Ceram. Soc. 93 (2010) 2783.

[12] R.P. Wang, H. Bando, T. Katsumata, Y. Inaguma, H. Taniguchi, M. Itoh, Phys. Status Solidi RRL 3 (2009) 142.

[13] R.Z. Zuo, C. Ye, X.S. Fang, Jpn. J. Appl. Phys. 46 (2007) 6733.

[14] Y. Uratani, T. Shishidou, F. Ishii, T. Oguchi, Jpn. J. Appl. Phys. 44 (2005) 7130.

[15] C.R. Zhou, X.Y. Liu, W.Z. Li, C.L. Yuan, G.H. Chen, J. Mater. Sci. 44 (2009) 3833.

[16] Z.H. Ren, G. Xu, X. Wei, X.H. Hou, Y. Liu, G. Shen, G.R. Han, Appl. Phys. Lett. 91 (2007) 063106.

[17] Y.G. Wang, G. Xu, X.P. Ji, Z.H. Ren, W.G. Weng, P.Y. Du, G. Shen, G.R. Han, J. Alloys Compd. 475 (2009) L25–30.